(14) Rept. no. MR 1471

NRL Memorandum Report 1471

FATIGUE CRACK PROPAGATION IN HIGH STRENGTH 4340 STEEL

(10) by

E. P. DAHLBERG
AND
D. B. LYTLE

METALLURGY DIVISION

(11) NOV 29 1963

(5)

U. S. NAVAL RESEARCH LABORATORY
Washington, D.C.

CONTENTS

Abstract ii
Problem Status ii
Authorization iii

INTRODUCTION 1

EXPERIMENTAL PROCEDURE 1

RESULTS 2

EFFECTS DUE TO CHANGES IN THE MAGNITUDE OF LOAD FLUCTUATION 4

CONCLUSIONS 6

REFERENCES 6

ABSTRACT

Fatigue crack propagation rates were measured in specimens of 4340 low alloy steel (yield strength 225,000 PSI) as a function of (1) the water vapor content of the fatigue environment and (2) the amount of fatigue load fluctuation. The fracture surfaces were analyzed by optical and electron microscopy, and attempts were made to correlate the observed fracture topography with the measured rates of crack propagation.

Both intergranular and transgranular fractures were observed in the regions of discontinuous crack growth. In several specimens the transgranular areas contained clearly defined parallel fatigue striations. Prior austenite grain boundary fractures were found in "flame" shaped areas at the crack origins. The combination of a high water vapor content and a low fatigue load fluctuation favored intergranular cracking while a low water vapor content and/or a high load fluctuation resulted in striation type fractures.

PROBLEM STATUS

This concludes one study in this problem. Work on other phases is continuing.

AUTHORIZATION

NRL PROBLEM NO. M01-08

~~BUREAU PROJECT NO. RRMA 02 091/652-1/R007 06 01~~

INTRODUCTION

A series of 3" wide Kahn type specimens of high strength 4340 low alloy steel were fatigue tested to failure in atmospheres containing various levels of water vapor. The main purpose of the series of tests was to determine what effect water vapor would have on the fatigue crack propagation rates. A secondary purpose was to generate a series of "pedigreed" fatigue fractures which could be analyzed by means of optical and electron fractography.

Understanding the correlation between a particular fracture structure and its propagating stress and environment is necessary for valid service failure analyses.

EXPERIMENTAL PROCEDURE

The specimens, 3" wide and 1/2" thick, were forged from 1-1/2" diameter AISI 4340 bar stock. After machining they were side-notched and fatigue pre-cracked to a depth of 1". The fatigue pre-cracking was carried out in approximately 100,000 cycles at a stress fluctuating between 2000 and 8000 lbs. The loading pin holes were located at the 1/3 position directly over the tip of the pre-crack. After pre-cracking, the specimens were austenitized at 1550°F, oil quenched, and tempered for one hour at 400°F. This heat treatment gave the material approximate yield and ultimate strengths of 225,000 PSI and 290,000 PSI respectively.

The water vapor content of the fatigue environment was controlled at three different levels. Compressed cylinder air was bubbled through water at 78°F and 32°F to produce approximate relative humidities of 80% and 20%. A third condition, nearly complete dryness, was produced by passing the compressed air through an anhydrone drying column.

The specimens were tested under tension-tension loading in a Sontag fatigue tester operating at 3600 cycles per minute. The maximum load for each specimen was set at 5000 lbs. The minimum load was varied from 1000 to 4000 lbs.

The crack depth was measured with a traveling microscope as a function of time. Crack growth rates at various crack depths could be determined from the slope of crack depth versus cycle curves plotted from this data. Using the stress intensity calibration curve prepared by A. M. Sullivan (1) for specimens with this geometry, the stress intensities corresponding to the maximum load at the different crack depths were calculated. Plots of crack growth rate versus maximum crack tip stress intensity were then prepared for each specimen.

RESULTS

Figure 1 presents a graph of the crack tip stress intensity versus growth rate for specimens tested in each of the three water vapor level environments. In each test the load varied from 5000 lbs maximum to 4000 lbs minimum. While the shape

of the three curves is generally the same, it is evident that at this low fatigue load fluctuation the crack growth rate for the specimen tested in a high water vapor environment was an order of magnitude greater than that for the specimen tested in a nearly dry atmosphere. Figure 2 shows macroscopic photographs of half of the fracture surfaces from each of these three specimens. The side-notch and pre-crack are on the left while the fast, unstable fracture region (beginning with the shear lip development) are on the right.

The region of discontinuous crack growth in the three specimens was characterized by a "flame" shaped area located at the base of the fatigue pre-crack. The size of this area diminished as the water vapor level was lowered. The test of specimen AT-44 [Figure 2(c)] extended over three working days. The hesitation type traces in this fracture are thought to be associated with the overnight interruptions in testing. Electron fractography showed the change in macroappearance of these "flame" regions to be associated with a change in the mode of fracture.

Figure 3 shows the fracture topography which developed in the flame shaped region at the very beginning of crack growth in specimen AT-42. It is distinctly intergranular. The fine detail on the grain facets, observed by stereographic viewing, consists entirely of ridges raised above the general

level of each grain. These tear ridges may result from a limited amount of ductility which accompanies the final stage of grain boundary separation. The details of tear ridge formation have been described by Beachem (2). The structure developed between the "flame" region and the area of fast fracture is shown in Figure 4. Although fatigue striations are not clearly resolved in this fractograph, the transgranular appearance and network of secondary cracking are characteristic of mechanical fatigue crack propagation in this material (3). The large arrow indicates the macroscopic direction of crack growth. Figure 5 shows the structure which developed in the fast fracture region. The fracture results from the coalescence of voids nucleating in front of the growing crack. The large dimples (arrows) may possibly be associated with grain boundary separation and subsequent deformation.

EFFECTS DUE TO CHANGES IN THE MAGNITUDE OF LOAD FLUCTUATION

Specimens were tested with various values of load fluctuation in both the high and the low water vapor environments. The maximum load on each specimen was 5000 lbs. The minimum load was varied from 1000 lbs to 4000 lbs. The results of these two series of tests are plotted in Figures 6 and 7.

In the dry atmosphere (Figure 6) the effects of changes in the load fluctuation are pronounced. A change in the growth rate of nearly two orders of magnitude accompanied a 5-1 to

5-4 change in the load fluctuation ratio. These large variations were not observed in the series tested in the high water vapor atmosphere. The growth rates in this instance (Fig. 7) were closer together. They were also approximately the same as the high load fluctuation tests done in the dry environment.

Figure 8 shows the fracture topography which developed approximately 0.60" from the tip of the fatigue pre-crack in specimen AT-46 which was tested with a 5/3 maximum-to-minimum load ratio in the dry atmosphere. The observed fatigue striations were not continuous over the entire surface but occurred in isolated patches, (arrows).

Fatigue striation spacings were measured at various crack depths on specimen AT-45 which was tested in dry air at a 5/1 load fluctuation ratio. Figure 9 shows a comparison of the observed crack growth rates and the striation spacing measurements. The maximum, minimum, and average striation spacing values are plotted together with the observed crack growth rate data. The close agreement of the two sets of data indicates that each striation results from a single stress cycle. Figure 10 shows several striations located at a depth corresponding to a stress intensity value of 46 KSI-$\sqrt{\text{INCH}}$.

CONCLUSIONS

Slow crack growth at the base of a sharp notch in this material can result from mechanisms of mechanical fatigue or atmospheric corrosion cracking. Under certain conditions combining low load fluctuation fatigue with reasonable levels of water vapor the rates of both mechanisms can be nearly identical. This situation can produce a fracture which will contain the characteristic features of both fracture modes. The range of stresses, strain rates, and water vapor environments used in this series of tests defines, to a limited extent, the conditions under which either of these mechanisms will operate. Additional tests are necessary to further define these growth rate parameters.

REFERENCES

1. A. M. Sullivan, "A New Specimen Design for Fracture Toughness", ASTM Materials Research and Standards (to be published).
2. C. D. Beachem, B. F. Brown, and A. J. Edwards, "Characterizing Fractures by Electron Fractography. Part XII. Illustrated Glossary, Section I: Quasi Cleavage", NRL Memorandum Report 1432, Jun 1963.
3. E. P. Dahlberg, "GASES IN STEEL [Characteristics of Fatigue Fractures]", Report of NRL Progress, pp 25-27, Apr 1963.

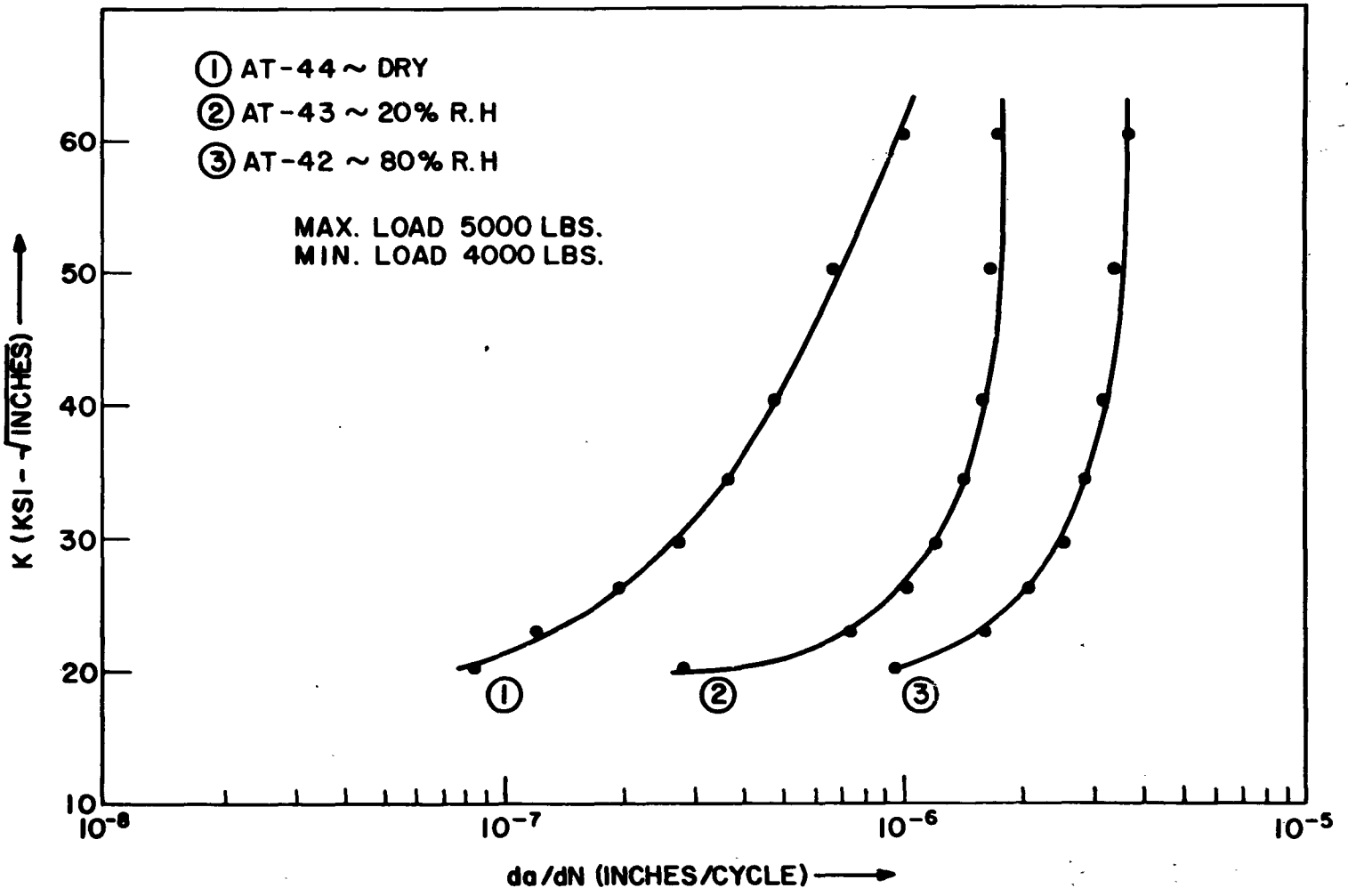

Figure 1 - Plot of maximum crack tip stress intensity (K) versus crack growth rate per cycle (da/dN) for three specimens tested in different water vapor level environments.

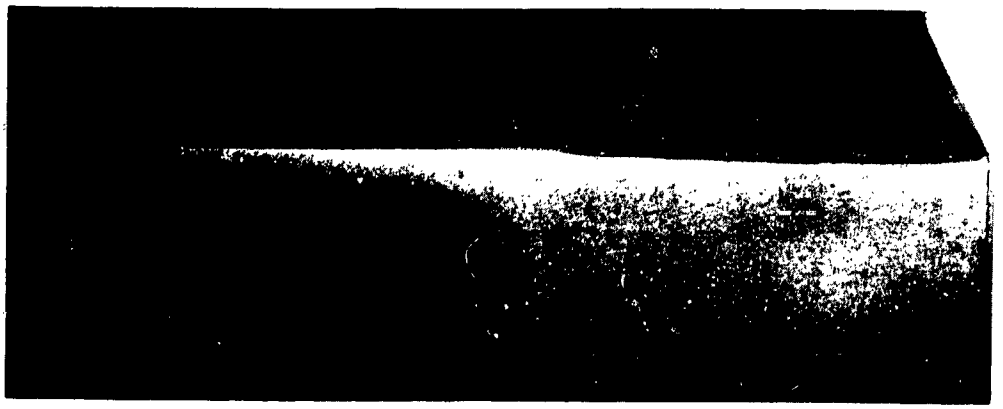

(A) AT-42

(B) AT-43

(C) AT-44

Figure 2 - The macroscopic appearance of fractures whose growth rates are plotted in Figure 1. Mag. 2.5X.

Figure 3 - Intergranular fracture observed in the "flame" shaped region of specimen AT-42. (a on Figure 2) Mag. 3000X.

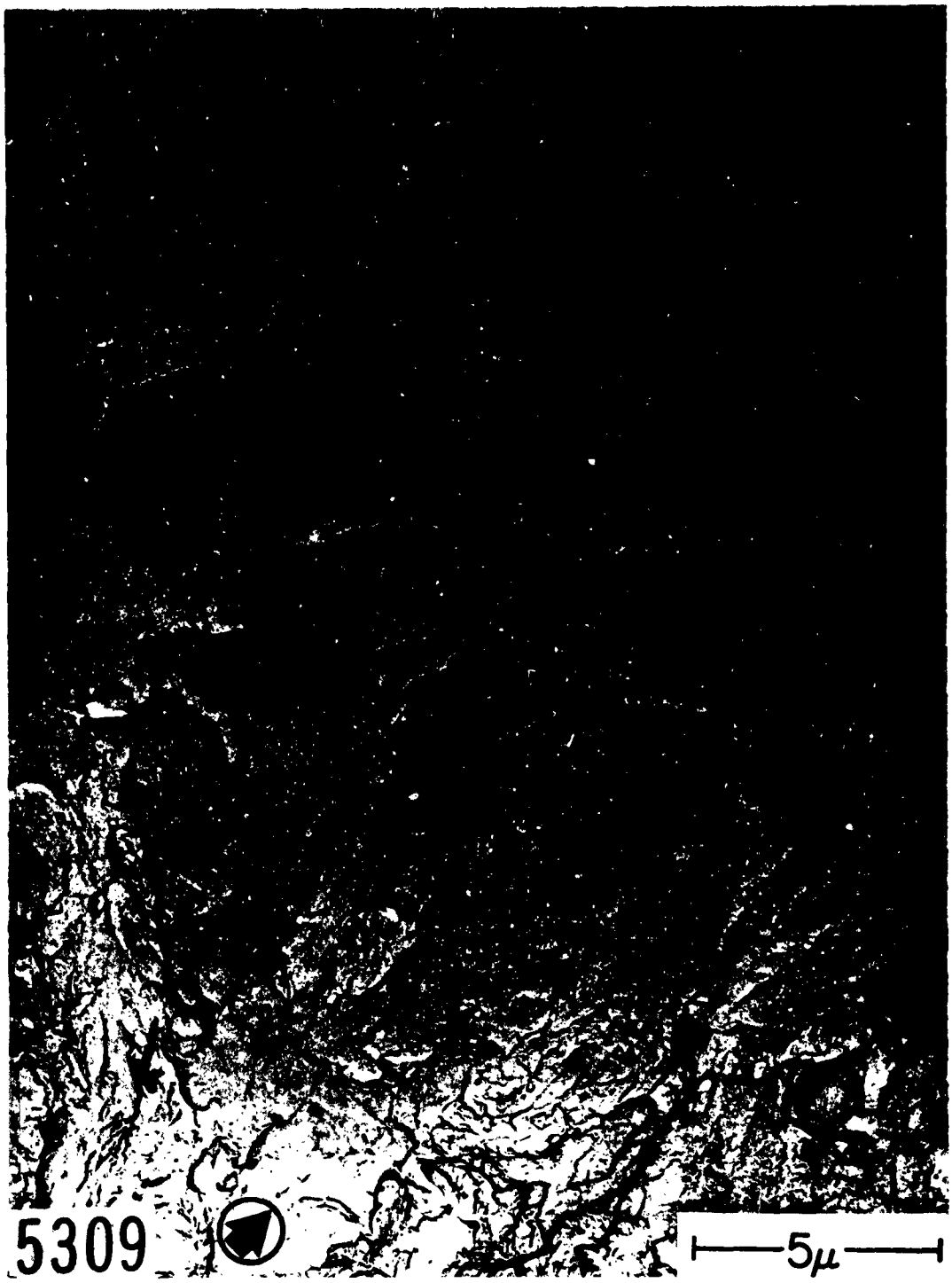

Figure 4 - Region of transgranular fatigue just prior to unstable crack growth in AT-42 (a on Figure 2). Mag. 9000X.

Figure 5 - Unstable fracture appearance in this alloy showing both large and small rupture dimples. Mag. 3000X.

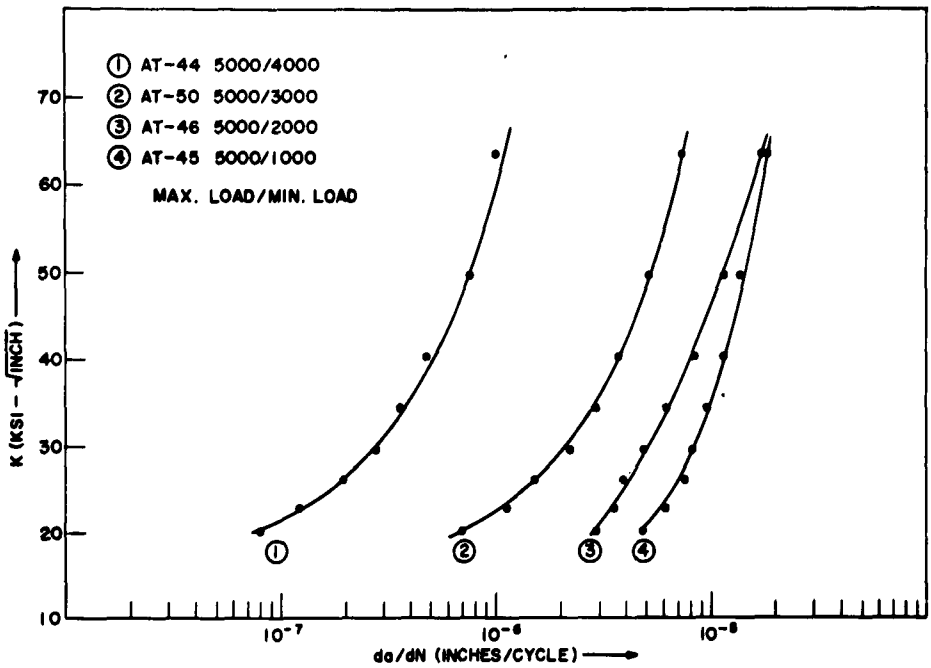

Figure 6 - Plot of maximum crack tip stress intensity (K) versus crack growth rate (da/dN) for series of specimens tested with different load fluctuations in a nearly dry environment.

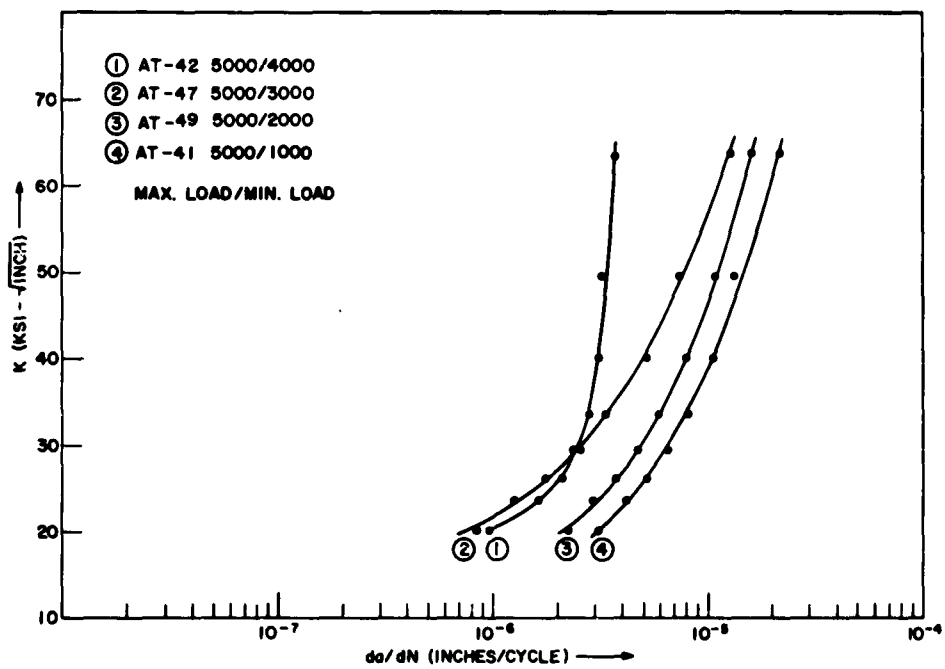

Figure 7 - Plot of maximum crack tip stress intensity (K) versus crack growth rate (da/dN) for series of specimens tested with different load fluctuations in a high (approx. 80% R.H.) water vapor environment.

Figure 8 - Region of transgranular fatigue in specimen AT-50 (dry environment, 5/3 load fluctuation) showing patches of parallel fatigue striations. Mag. 6000X.

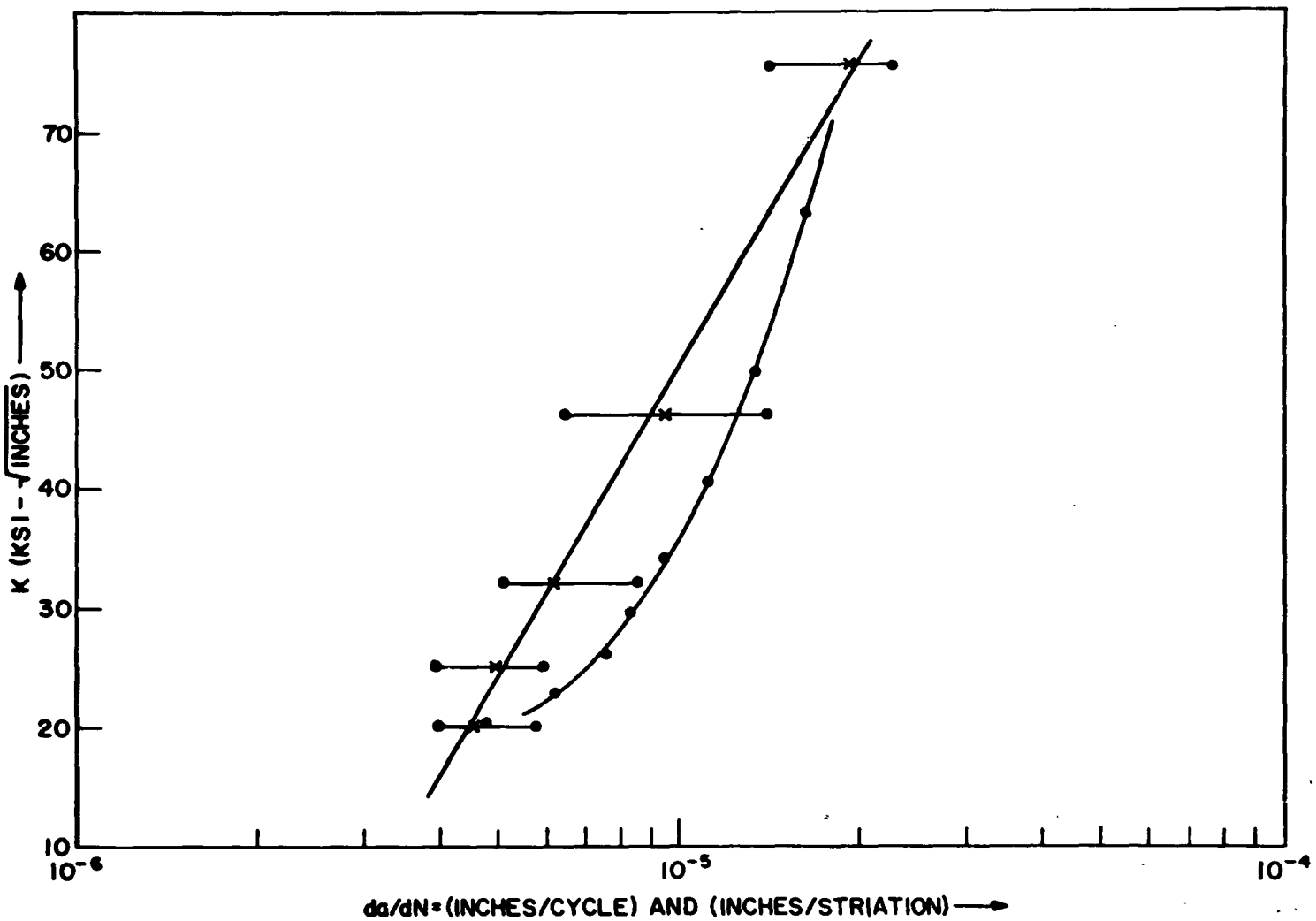

Figure 9 - Comparison of the observed crack growth rate (da/dN) and the measured striation spacing for specimen AT-45 (dry environment, 5/1 load fluctuation).

Figure 10 - Patch of parallel fatigue striations located on the surface of specimen AT-45 at a depth corresponding to a stress intensity of 46 KSI $\sqrt{}$ INCH. Mag. 30,000X.